

Spectroscopic Studies of Photodegradation of Polyethylene Films Containing TiO₂ Nanoparticles

Rui Yang,¹ Paul A. Christensen,² Terry A. Egerton,² Jim R. White,² Adam Maltby³

¹Department of Chemical Engineering, Tsinghua University, Beijing 100084, China

²School of Chemical Engineering and Advanced Materials, Newcastle University, Newcastle upon Tyne NE1 7RU, United Kingdom

³CRODA Chemicals Europe, Ltd., Oak Road, Hull HU6 7PH, United Kingdom

Received 9 July 2009; accepted 27 September 2009

DOI 10.1002/app.31669

Published online 18 August 2010 in Wiley Online Library (wileyonlinelibrary.com).

ABSTRACT: The effect of UV radiation on a family of low density polyethylene films containing different concentrations of TiO₂ nanoparticles has been studied. The photodegradation was monitored using FTIR measurements of carbonyl group development and an *in situ* FTIR method that tracks the generation of CO₂ as a principal product of degradation. Samples containing dispersant and/or a phenolic antioxidant but free from TiO₂ particles were examined as controls. It was shown that the effects of photodegradation of the polymers could be followed even when these additives were present. The dispersant gave rise to absorption in the carbonyl region of the IR spectrum but meaningful results concerning the progress of photodegradation were obtained using difference spec-

tra. Good correlation was found between the carbonyl and the CO₂ measurements of the relative photosensitivities of the films with different compositions, and both methods indicated that addition of the nano-particulate rutile TiO₂ had decreased the film photostability. The decreased photostability inferred from spectroscopic measurements was also observed as a reduction, from ~ 1100 h to 400 h, of the exposure time before film cracking, when samples were exposed to UVA radiation in QUV equipment. © 2010 Wiley Periodicals, Inc. *J Appl Polym Sci* 119: 1330–1338, 2011

Key words: polyolefins; titanium dioxide; nanoparticles; FT-IR; photodegradation

INTRODUCTION

Commercial polymeric materials usually contain a variety of additives. These include both molecular and particulate antioxidant stabilizers, which are included to protect the material during both processing and service. Fibers and particles are often added to improve the material's mechanical properties, and for the past 20 years, nanoparticles have been increasingly used to enhance these properties at lower mass fractions than are used for macroscopic fibers and particles.^{1–9} The introduction of any particulate additive almost inevitably demands the use of a dispersant to prevent particle aggregation.

This article is concerned with TiO₂ nanoparticles. Because of their small size, these nanoparticles can be used to modify the film properties without sacrificing film transparency but, because TiO₂ is a broad band semi-conductor, they absorb short wavelength light. Consequently, they offer a way to tailor the

optical properties of the polymer nanocomposite. For example, packaging film could have sufficient transparency to let the wrapped contents be seen, but still prevent the photochemically active wavelengths from reaching and spoiling the product. By acting as a UV screen, the TiO₂ may protect the polymer from photochemical degradation and lengthen its lifetime. Conversely, it may instead shorten film lifetime by photocatalyzing polymer degradation. Indeed, photocatalysis has been studied as a method of disposing of used plastics articles, especially for poly(vinyl chloride).^{10–12} Aspects of the photoprotection and photosensitization of polyolefins by TiO₂ have been discussed by the current authors¹³ and by Allen and coworkers.^{14–18} The latter workers concluded that nano-particle TiO₂ was generally more active than pigmentary (~ 0.3 μm) TiO₂^{16,17} and that for polyethylene (PE) filled with 0.5% TiO₂, the time to reach a carbonyl index of 0.1 was greater for 25 nm rutile than for 20–30 nm anatase, and that this time varied with particle size for different nano-anatase powders.¹⁶ However, as the coating applied to TiO₂ pigments strongly influences the balance of photocatalysis and photoprotection,^{16,17,19} it is very difficult to decouple any intrinsic size-related effect from the effect of the coating on the nanoparticles. Zeynalov and Allen showed that nano-titania (and particularly nano-rutile)

Correspondence to: T. A. Egerton (T.A.Egerton@ncl.ac.uk).

Contract grant sponsors: China Scholarship Council, UK DTI/EPSRC (ACORN Collaborative Project with Croda Chemicals).

reduced the efficiency of a hindered amine light stabilizer.¹⁸ They examined the influence of the various particles on the efficiency of the phenolic antioxidant, Irganox 1010,¹⁹ and commented that the high surface-to-volume ratio of nanoparticles would be expected to enhance any surface-supported (catalytic) reactions such as those involved in polymer oxidation.

As it is not always possible to predict whether photocatalysis or photoprotection will prevail, and because molecular additives, such as, dispersants or thermal stabilizers can potentially interact with the nanoparticles in either a beneficial or harmful way, the design of such PE-TiO₂ nanocomposite films requires a significant program of experimentation. In particular, any polymer formulation that will be exposed to UV in service must be tested for its susceptibility to photo-oxidation. Many laboratory-based methods for accelerated testing exist,²⁰ but most of them require many weeks of UV exposure to provide meaningful data and this seriously impedes product development. Allen et al. experimented with the use of microwave photodielectric spectroscopy to determine the relative photoactivities of their semiconducting particles,^{16,17} but their method does not give information that is specific to a particular polymer substrate. The current workers developed a method in which the carbon dioxide generated by photo-oxidation is monitored and used to compare the UV degradation rates of different polymer compounds.^{13,21–24} Using this method, the relative photocatalytic activity of a pigmentary grade of TiO₂ could be assessed after 3–5 h UV exposure.^{13,21} The extension of this method to films with low levels of nano-particulate TiO₂ must take into account that such films only partly attenuate the incident irradiation. They are unlike either unpigmented PE, in which the photochemically active UV wavelengths are only weakly absorbed, or pigmented PE films in which the UV is absorbed in a very short distance.²⁵ Therefore, to test the applicability of the carbon dioxide photogeneration method, CO₂ results have been compared with results from the widely used carbonyl development method. In addition, these spectroscopic studies have been complemented by measurements of film weight loss and film cracking.

EXPERIMENTAL

TiO₂ nanoparticles

The nano-particulate rutile TiO₂ was an experimental material prepared by Croda Chemicals by hydrolysis of TiCl₄ and was surface treated with a coating which consisted essentially of aluminum and stearate species. Characteristics of a similar material

have been reported previously.²⁶ The surface area (BET, N₂) of the uncoated TiO₂ was ~ 130 m²/g, which corresponds to an equivalent sphere diameter of 10 nm. This is broadly consistent with an X-ray line-broadening size of ~ 7 nm measured perpendicular to the [110] crystal planes. Transmission electron micrographs showed the particle to be acicular, measuring ~ 15 nm × 75 nm with the crystallographic *c*-axis oriented along the length of the crystal. By contrast, the particles used in Allen et al.¹⁷ appear to have been prepared by precipitation from titanyl sulfate solution and are, therefore, presumed to have a different morphology.

The polymer

The low density polyethylene (LDPE) films containing nano-particulate TiO₂ and the associated control films were made from Basell Lupolen 2420H LDPE, the melt flow index of which is 1.9 g/10 min.

Film composition and preparation

LDPE masterbatches containing the appropriate additives, for example, 5% of a liquid dispersion of TiO₂ and 2% Irganox 1010 antioxidant, were prepared from the "Parent" Basell LDPE using a counter-rotating twin screw extruder run at 180–185°C and fitted with a single strand die. The strands were cooled in water and then pelletized. Amounts of masterbatch calculated to give the desired final level of additives were then "let down" with the same 2420H polymer, using the same extruder temperatures but with the strand die replaced by a film die. The extruded film was cooled on rollers chilled to 10°C before collection on a reel.

All films were 100 μm thick. Their compositions are listed in Table I. For convenience, films contain-

TABLE I
Compositions of the Films

Film number and designation	Loading (%) of nano-particulate TiO ₂	Loading (%) of Irganox 1010	Dispersion/dispersant carrier
88, Parent	0	0	None
89, T1	0.25	0	C1
90, T2	0.75	0	C2
93	0	0.075	None
94	0.25	0.075	C1
95	0.75	0.075	C2
102	0	0	C1
103	0	0	C2

The same liquid dispersion and dispersant was used throughout, but different amounts, proportional to the TiO₂ loading, are designated C1 and C2. Films 102 and 103 were controls formulated without TiO₂, but with the same dispersion/dispersant carrier.

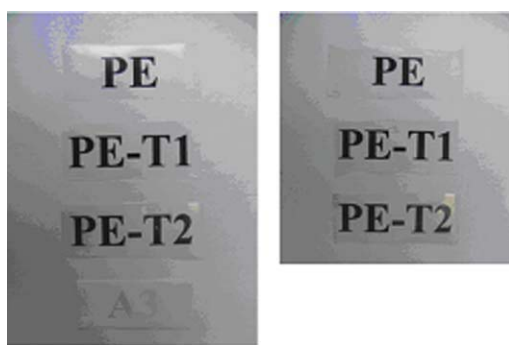


Figure 1 (a) An illustration of the difference in transparency of PE, PE-T1, PE-T2, and A3. Strips of these films were placed over a sheet of paper printed with the appropriate film code. It is evident that the A3 film is almost opaque. (b) A similar transparency assessment for PE, PE-T1, and PE-T2 after 581 h UV exposure. Small changes in transparency have occurred. [Color figure can be viewed in the online issue, which is available at wileyonlinelibrary.com.]

ing 0.25% and 0.75% nano-particulate TiO₂ are often designated "T1 and T2" respectively, in the subsequent text. Because the films containing nano-particulate TiO₂ were formulated with an undisclosed dispersant package, control films #102 and #103 were prepared without TiO₂ but with an amount of dispersant corresponding to that used for the 0.25% and 0.75% TiO₂ films, respectively. Some films, #94 and #95, were formulated with both TiO₂ and 0.075% Irganox 1010 stabilizer. Once again, a control film without TiO₂ was prepared (#93 in Table I). In addition to the samples listed in Table I a further film, made from a different LDPE, and containing 5% of anatase with a crystal size of $\sim 0.15 \mu\text{m}$ was used for comparison purposes; it is designated "A3." This material has been used in other studies in this laboratory and is used as a standard to check instrumental response, for example, when the illuminating UV lamp is changed, as well as acting as a comparator for the nanocomposites. As shown in Figure 1, the as-prepared films containing nanoparticles were highly transparent, whereas the A3 film was translucent.

Measurement of CO₂ photogeneration

The measurements of CO₂ generation were conducted using a specially constructed cell that is described elsewhere.^{13,21–24} LDPE films in the form of disks were placed in the cell and held against a magnetic disk by a metal ring (8 mm i.d.). Before measurements began, the cell was flushed for an hour with cylinder oxygen [$\leq 30\%$ relative humidity (RH)], or with humidified oxygen that had been bubbled through saturated NaNO₂ solution ($\sim 66\%$ RH) or through deionized water ($\sim 100\%$ RH).

Unless otherwise indicated, the cell was flushed with high humidity oxygen in the tests reported below. The cell was then isolated and positioned in the sample compartment of a Bio-Rad FTS-60 spectrometer, which was fitted with a high sensitivity, narrow band, liquid nitrogen-cooled mercury cadmium telluride (MCT) detector. The spectrometer was then purged with nitrogen until the spectrum showed that the levels of both water and carbon dioxide were constant.

Before irradiation, spectra were recorded at 20 min intervals for 1 h to ensure that the level of CO₂ was constant and low. Irradiation was then begun using the broad band output ($\sim 280\text{--}800 \text{ nm}$) from a 150 W high-pressure xenon arc lamp (Oriol) filtered by 100 mm of water, to reduce IR heating, and by an AM0 solar filter to remove wavelengths below 290 nm. The spectral distribution of the radiation falling on the sample has been reported previously.¹³

During irradiation, the build up of carbon dioxide within the cell was followed by monitoring an absorption centered at 2360 cm^{-1} and attributed to the asymmetric stretching vibration of CO₂. All spectra (100 co-added and averaged scans) were run at 4 cm^{-1} resolution. Irradiation was stopped after 3 h and the carbon dioxide was monitored for a further hour.

Carbonyl development and mass changes in films exposed to UVA340 radiation

Films were exposed to UV radiation from UVA340 tubes in a QUV accelerated weathering tester (Q-Panel Company, Cleveland, OH) operated at 40°C without temperature or humidity cycling. The UV tubes were cycled every 400 h according to the manufacturer's recommendation. The integrated area of the carbonyl region ($1775\text{--}1680 \text{ cm}^{-1}$) was used as the measure of carbonyl formation. In some cases, overlapping absorptions due to the presence of different types of carbonyl group were observed. Where appropriate the exact peak position was obtained from the second derivative of the absorption curve and the overlapping bands in the region $1600\text{--}1850 \text{ cm}^{-1}$ were deconvoluted using the "Peak Resolve" function in OMNIC software (Thermo Electron Corporation) to give the peak position, height, and peak area of each band.

During UV exposure, duplicate films of each sample were weighed every about 80 h on a Mettler Toledo B204-S balance with a precision of 0.1 mg. The averaged masses for each sample were compared with the mass of control samples kept in a "dark" place and weighed at the same time. Surgical gloves were used to avoid any contamination from fingers.

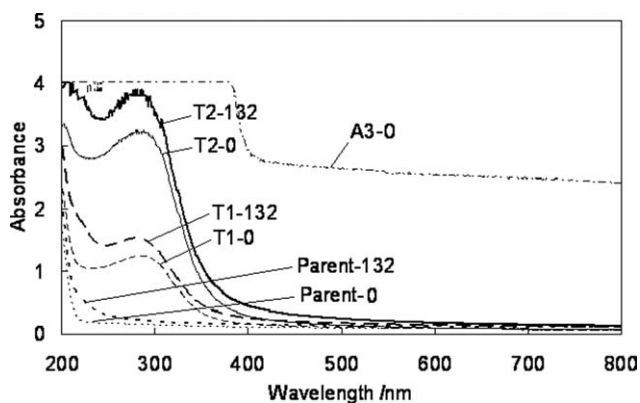


Figure 2 The transmission of the Parent, T1, and T2 films before and after 132 h exposure to UV radiation. The transmission of film A3 is shown for comparison.

RESULTS

UV and visible light absorption

TiO₂ absorbs UV, which excites electrons from the valence band to the conduction band. The UV-visible spectra for films of the parent LDPE and the derived T1 and T2 films containing nano-particulate TiO₂ are compared with that of A3 in Figure 2. The lower limit of the filtered output from the xenon lamp occurs near 300 nm. Figure 2 shows that at 300 nm, the initial absorbance, A , of the 0.25% TiO₂ (T1) film is ~ 1.2 . The fraction (I/I_0) of radiation reaching the rear of the film, calculated from the equation $\log_{10}(I_0/I) = A$, was 0.063, about 6%. At the same wavelength, the nominal absorbance (~ 2.9) of the 0.75% TiO₂ (T2) film indicates that only 0.1% of the radiation reaches the “dark” surface. Thus, although the T1 and T2 films do not absorb as strongly as A3, both films significantly attenuate UV, even at these low TiO₂ loadings. The spectra also show that LDPE, T1, and T2 are essentially transparent to visible light, whereas film A3 is essentially opaque.

During QUV exposure, the UV absorption spectra of the parent LDPE and of films T1 and T2 changed as is shown in Figure 2. One consequence of the changes is increased absorption of the 300–350 nm component of the xenon lamp output.

Measurements of film photostability by carbonyl group development

Effect of carrier package

The IR spectra from 1675 to 1800 cm⁻¹ of unexposed films are shown in Figure 3. A weak but significant absorption at ~ 1750 cm⁻¹ increased with the amount of dispersant (the carrier package), but was unaffected by the presence of 0.075% Irganox 1010. The absorption in this region of the spectrum increased when films were exposed to UV, as is

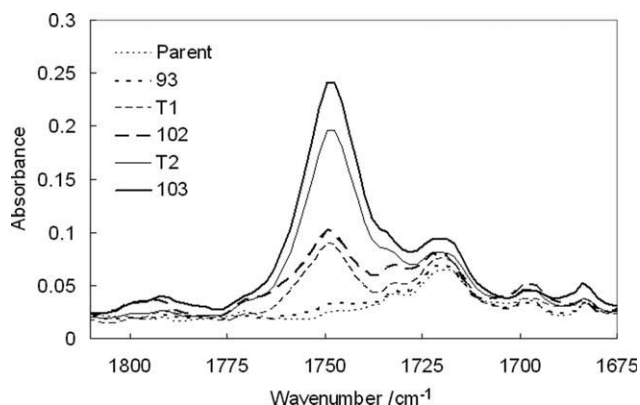


Figure 3 Infrared spectra in the carbonyl region of LDPE films before UV exposure.

shown in Figure 4 for the Parent film. Exposure gave a sharp but weak absorption at ~ 1640 cm⁻¹ attributed to the formation of vinyl groups.²⁷ More strikingly, UV exposure also led to development of an increasingly strong absorption at 1711 cm⁻¹ and subsequent development of shoulders near 1728 cm⁻¹ and 1780 cm⁻¹ (Fig. 4). The integrated intensities of the absorption are shown for parent LDPE and #102 and #103 films, formulated with dispersant only, as function of exposure time (Fig. 5). The similarity of these three plots indicated that the dispersant did not, by itself, greatly affect carbonyl development. Therefore, carbonyl development was monitored by subtracting initial spectra from the spectra of exposed films.

Effect of incorporation of nano-particulate TiO₂

Exposure of the TiO₂-containing films, T1 and T2, led to absorption at 1711 cm⁻¹ which was similar, though stronger, than that found for the film formulated without TiO₂. Again shoulders developed near

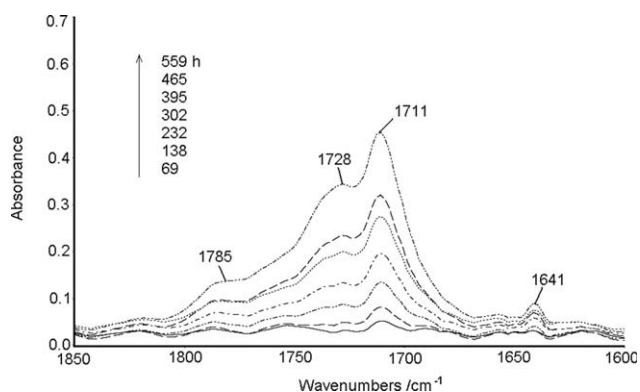


Figure 4 Development of carbonyl absorption during QUV exposure of the parent LDPE. Spectra are presented relative to those of unexposed film.

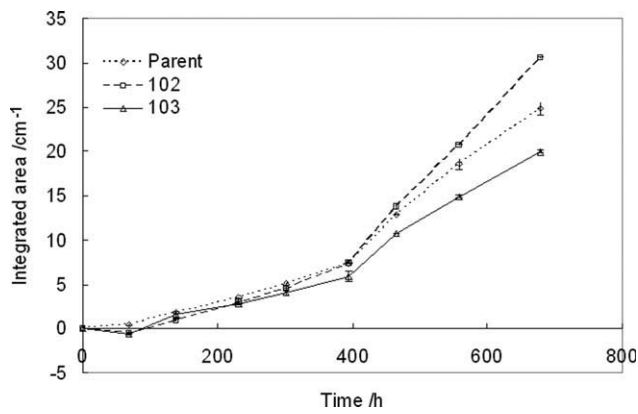


Figure 5 The increase in carbonyl absorption during UV exposure of the Parent LDPE and of control films 102 and 103 formulated with different levels of dispersant.

1730 cm^{-1} and 1780 cm^{-1} [Fig. 6(a)]. In addition, at long irradiation times, the 1711 cm^{-1} absorbance weakened and an additional shoulder grew at $\sim 1719\text{ cm}^{-1}$. Deconvolution of the T2 spectrum between 1650 cm^{-1} and 1800 cm^{-1} [Fig. 6(b)] confirms the composite nature of the absorption band and revealed an apparent small shift in the positions of some peaks, for example, a shift of the shoulder

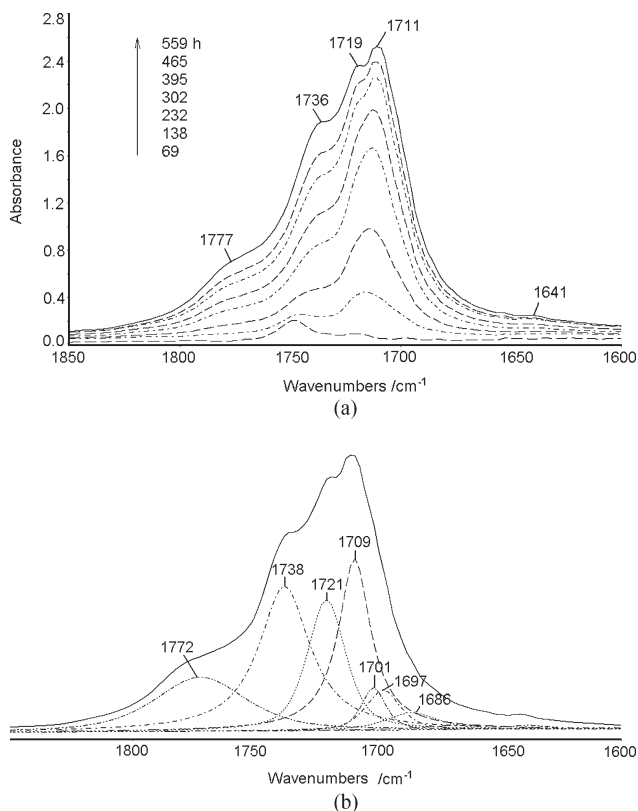


Figure 6 (a) Development of carbonyl absorption during QUV exposure of the T2 film (0.75 TiO_2). Spectra are presented relative to those of unexposed film. (b) Deconvolution of carbonyl spectral peak for T2.

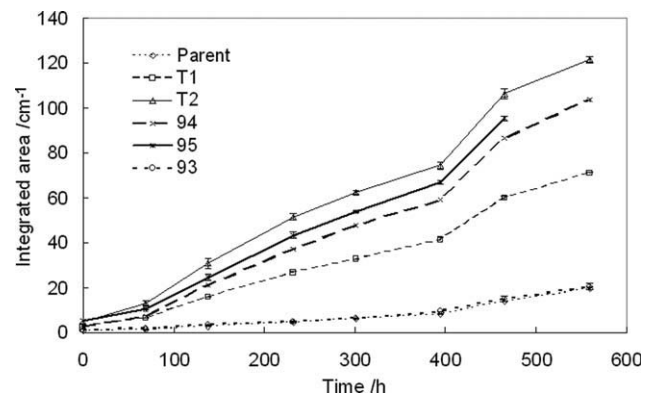


Figure 7 Increase in carbonyl absorption (integrated between 1680 cm^{-1} and 1775 cm^{-1}) in LDPE films containing 0%, 0.25%, and 0.75% nano-particulate TiO_2 . Results for TiO_2 films with (94 and 95) and without (T1 and T2) additions of 0.075% Irganox 1010 are compared. Note that the results for LDPE Parent and LDPE Parent + Irganox 1010 (#93) superimpose almost exactly.

at $1719\text{--}1721\text{ cm}^{-1}$. As the initial spectra were recorded at a resolution of 4 cm^{-1} , this shift was considered not to be significant. In Figure 7, the integrated absorbance between 1680 cm^{-1} and 1775 cm^{-1} is plotted as a function of irradiation time for Parent, T1 and T2 films together with the results for the films #93, #94, and #95 in which 0.075% Irganox is also present. The key conclusion is that addition of the nano-particulate TiO_2 has decreased the photostability of the film.

Film embrittlement and weight loss

During the course of the QUV exposure, the films became brittle and cracked. Because the films were inspected at intervals of $\sim 80\text{ h}$, the recorded cracking time, t_c , may be an overestimate. The critical condition might have been reached at any time during the previous exposure interval. In Figure 8, the

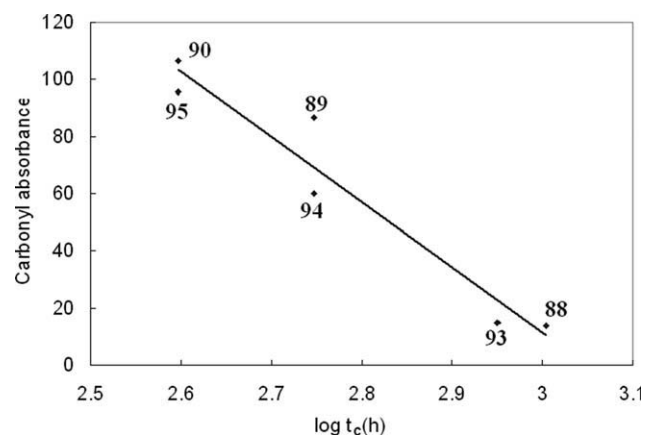


Figure 8 Carbonyl absorbance after 465 h exposure versus the time to cracking (t_c) in hours, plotted as $\log t_c$. The best fit straight line is shown ($R^2 = 0.935$).

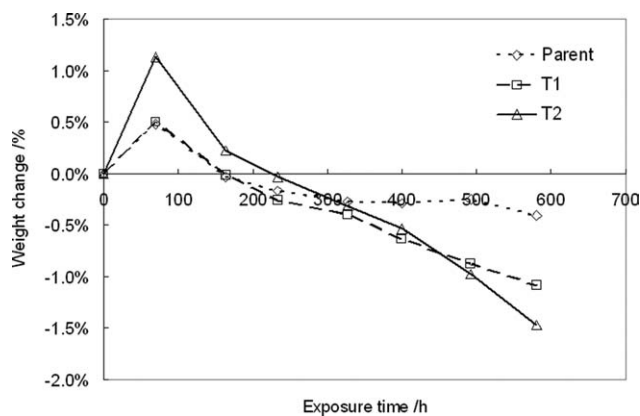


Figure 9 Weight changes recorded for LDPE Parent, T1, and T2 films during exposure to UVA340 irradiation.

carbonyl absorption values after 465 h UV exposure are plotted against the time to cracking, t_C , for films with and without Irganox thermal stabilizer. To a good approximation, they varied linearly with the logarithm of the cracking time.

The film weight changes recorded during the course of the QUV exposure are shown in Figure 9. Initially, the film increased in weight, presumably because the polymer incorporates oxygen as a charge transfer complex, perhydroxyl, or carbonyl.²⁸ Later, the weight falls, presumably because the polymer degrades to volatile products, such as, carbon dioxide.

Spectrometric monitoring of carbon dioxide photogeneration

The increases in gas-phase carbon dioxide monitored during irradiation of LDPE films, with and without TiO₂, are compared in Figure 10(a,b). Films T1 and T2 contained 0.25% and 0.75% TiO₂, respectively, and also dispersant. However, the results in Figure 10(a) show that neither the addition of the carrier C2 nor the addition of Irganox 1010 to the parent LDPE affect CO₂ photogeneration. In all cases, the absorbance of CO₂ increased immediately when radiation began, and essentially stopped increasing when radiation ceased. The rate of CO₂ generation was lowest for Parent LDPE. The sample containing pigmentary anatase TiO₂ (A3) gave a significantly higher rate, consistent with previous studies on pigmented PE films.¹³ The rates of CO₂ generation for the films containing nano-particulate rutile TiO₂ were even greater. For all samples the CO₂ absorbances increased linearly over the 3 h of UV exposure and the rate increased from 0.49–1.0 to 1.5×10^{-4} a.u. min⁻¹ as the nano-particulate TiO₂ loading increased from 0–0.25% to 0.75%. It is noted that in the earlier studies of pigmentary TiO₂, the A3 films gave much

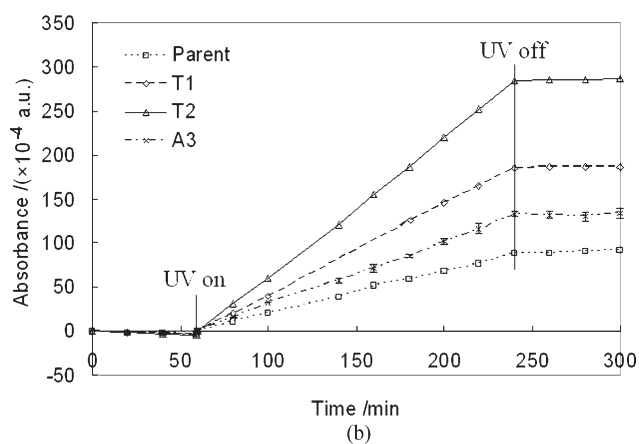
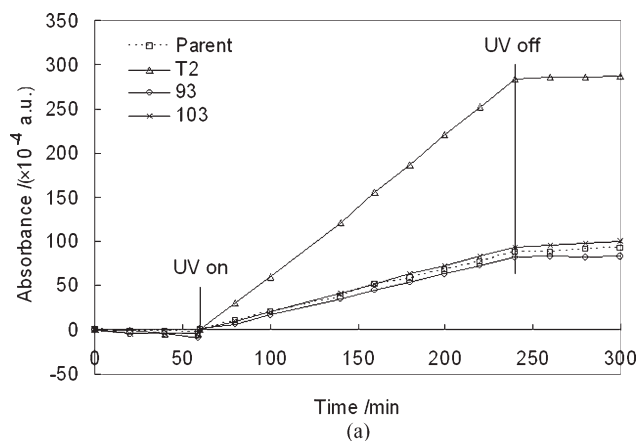


Figure 10 Photogeneration of CO₂ during irradiation of LDPE. (a) A comparison of the effect of 0.75% TiO₂ with the effect of either Irganox (#93) or dispersant (#103). (b) The effect of pigmentary anatase, and of 0.25% and 0.75% nano-particulate TiO₂.

higher CO₂ emission than films containing various rutile pigments.

The results in Figure 11 show that the amount of photogenerated CO₂ increased with increasing

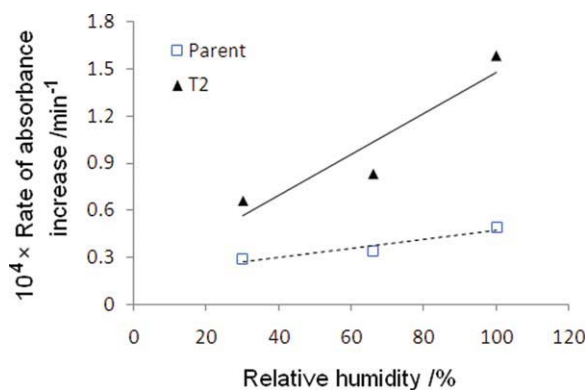


Figure 11 Dependence of the rate of CO₂ photogeneration from Parent and T2 LDPE films in oxygen atmospheres on the humidity of the oxygen. [Color figure can be viewed in the online issue, which is available at www.interscience.wiley.com.]

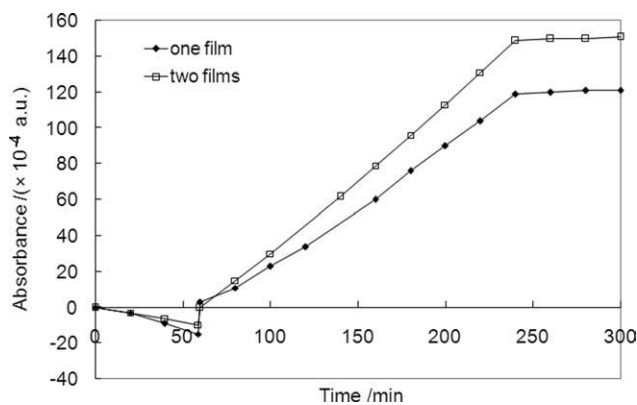


Figure 12 Photogeneration from two T2 films, one placed behind the other.

humidity as found in previous studies^{13,23} and that, at all humidities, the addition of nano-particulate TiO₂ increased the CO₂ photogeneration. When two T2 films were stacked together to form a sample with twice the standard thickness, the CO₂ absorbance at the end of 3 h UV irradiation in dry oxygen was 149 compared with 119 with a single film (Fig. 12). This increase by a factor of ~ 1.3 is less than the doubling that was found for similar studies with unpigmented LDPE film.¹³

DISCUSSION

Absorption of UV

Direct spectrometric measurements of UV attenuation showed that $\sim 99\%$ of the 300 nm radiation was absorbed within the thickness of the films containing 0.75% nano-particulate TiO₂. The absorption of the photoactive UV by T2 films is demonstrated by the fact that the total photogeneration of CO₂ from two T2 films stacked on top of one another was 130% that from a single film, which implies that the degradation of the second film is only 30% that of the front one. This implies that the front film attenuates the UV, which is active for polymer degradation by $\sim 70\%$. The difference between the 70% attenuation of active UV inferred from CO₂ experiments and the spectrometric measurement of 99% attenuation at 300 nm implies that photodegradation of films containing nano-particulate TiO₂ is activated by wavelengths greater than 300 nm, where the film absorbs less strongly. The results support the view that heterogeneous photocatalysis by the TiO₂ makes a major contribution to the degradation of the nanocomposite films by wavelengths in the 300–380 nm range.

During exposure of the films to UVA their absorption near 300 nm increased. The films remained transparent to visible light, as is shown by Figure 1,

and this indicates that the photochemical changes are not due to production of long chain conjugated polyenes, which would absorb in the visible region. Although the absorption is too broad to permit precise assignment of the changes, as is usual with UV spectra, it probably reflects the incorporation of chromophores based on the carbonyl groups, of which its presence is unambiguously shown by IR analysis.

The effect of additives

Before considering the usefulness of spectroscopic measurements as indicators of the effect of nano-particulate TiO₂ on the photostability of LDPE films, it is helpful to understand the effect of the antioxidant and "carrier" additives on these measures of photostability. As part of this process, measurements were made on control films prepared with the antioxidant or the dispersant used in the preparation of the nanocomposites, but without TiO₂. Films formulated with 0.075% of Irganox 1010 did not absorb significantly in the carbonyl region of the IR spectrum and showed only small differences in the development of carbonyl absorption during subsequent UV exposure. After 700 h UV exposure, the integrated carbonyl signals for the parent polymer and for the "parent plus carrier" all fell within the range $25 \text{ cm}^{-1} \pm 5 \text{ cm}^{-1}$. (For comparison, the corresponding value for T2 was $\sim 120 \text{ cm}^{-1}$). The dispersant absorbed in the carbonyl region of the IR spectrum but meaningful data were obtained by subtracting the starting spectra from the corresponding spectra obtained after UV exposure. It is concluded that neither the dispersant nor the antioxidant affects the carbonyl measurement of polymer degradation. Similarly, the results in Figure 10 show that neither the addition of 0.075% Irganox nor the additions of the dispersant package C2 to the Parent LDPE film affected the photogeneration of carbon dioxide.

Spectrometric measurements of changes in film composition

The good correlation of the integrated absorbance due to carbonyl groups, measured after 465 h with the time at which film cracking was first observed (Fig. 8) indicates that, for the family of materials investigated here, the FTIR carbonyl signal satisfactorily tracks a mechanical property that is of importance for this class of film. The results in Figure 8 include films both with and without thermal stabilizer, and this implies that this relevance of the spectrometric method of monitoring the degradation is independent of the presence of the Irganox stabilizer. Further, as discussed in previous section (The effect of additives), the results in Figure 5 show that

the development of carbonyl absorption in these films is not significantly affected by the presence of dispersant C. However, the results in Figure 7 imply that although the addition of 0.075% Irganox to film T2 (with 0.75% TiO₂) has little effect on carbonyl development, its addition to T1 (with 0.25% TiO₂) accelerates carbonyl development. This sensitivity of carbonyl development to the details of the pigment is paralleled in results of Allen et al. They found that, for a 200- μm polypropylene film with 0.1% Irganox 1010, addition of 0.5% of a polysiloxane coated rutile pigment increased by 50% the time to reach a carbonyl index of 0.06. By contrast, addition of an uncoated anatase decreased this time by 50%.²⁹ Results of a study of a model reaction, cumene oxidation, were interpreted as suggesting that nano TiO₂ increased the rate of initiation of thermal oxidation and that the effects were greater for rutile than anatase.¹⁹ The contrast between these two sets of results illustrates the difficulty in discerning simple behavior patterns. Because the influence of TiO₂ on the model oxidation of cumene increased with its surface area, Allen and coworkers emphasized the possible importance of surface interactions.

An alternative, though speculative, hypothesis is that the TiO₂/Irganox interaction is photochemical in origin and that when UV penetrates throughout the film all of the Irganox may interact with the TiO₂. This could be the case for the anatase and the very small (high area) nanoparticles studied by Allen and coworkers or for the T1 (0.25% TiO₂) results reported earlier. However, when UV is screened more strongly, by rutile rather than anatase,²⁹ by slightly larger nanoparticles rather than the very smallest,¹⁹ or by the more highly loaded T2 films reported earlier, the UV flux within the film core could be much smaller, and consequently, any photoreactions of Irganox with TiO₂ would be reduced. Significant further work including careful optical measurements would be needed to test this hypothesis.

Taken as a whole, the results imply that the development of carbonyl absorption can give a useful indication of the photostability of films formulated with nano-particulate TiO₂.

Despite the broad similarity of the FTIR spectra of the various compositions, both before and after UV exposure, there are differences between the carbonyl spectra of the parent films and those containing nano-particulate rutile. The relative proportions of the different absorptions contributing to the "carbonyl absorption" are shown in Figure 13, which suggests that the relative importance of the different species is different in the parent and TiO₂-containing LDPE films. Spectral deconvolution suggests that the main absorptions occur near 1701, 1709, 1721, 1738, and 1772 cm⁻¹. Absorption at the lower frequencies

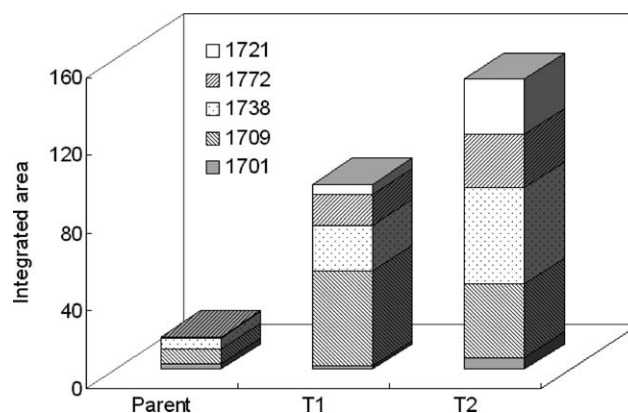


Figure 13 The integrated areas of absorptions of different carbonyl species with peaks at the given wavenumber positions for the Parent, T1, and T2 films.

has been attributed to carboxylic acid and ketones.^{30,31} The acids can react with hydroxylated groups to form linear or cyclic esters responsible for IR absorptions near 1738 cm⁻¹ and 1770 cm⁻¹, respectively.³¹ It appears that the ratio of acid to (linear and cyclic) esters is smaller in the parent LDPE than in T2, and the implications of these differences will be discussed in the subsequent article.

Photogenerated CO₂ as a rapid indication of the effect of nano-particulate TiO₂ on film photostability

Although there was a good correlation between development of carbonyl absorption and "time to crack," the uncertainties indicated in the previous section show the potential benefits of a speedier measure of photoactivity. The weight measurements reported in Figure 9 showed an initial increase of between 0.5% and 1%, which was attributed to the uptake of oxygen. Subsequent weight losses are attributed to the loss of volatiles caused by chain scission, for which the ultimate product is CO₂. This study has shown that the photogenerated CO₂ can be measured after 3 h UV exposure, and in Figure 14, the CO₂ results are shown to correlate with the widely used carbonyl absorbance measurement.

Unlike the weight loss measurements or the development of carbonyl absorption, the measurement of CO₂ photogeneration can be monitored in just a few hours, as shown in Figure 10.

Sensitivity of CO₂ measurement was not a problem in the present investigation because of the strong degradation of LDPE under the conditions applied. If very small amounts of CO₂ are predicted, the measurements should be carried out in humidified oxygen because this enhances the amount generated.

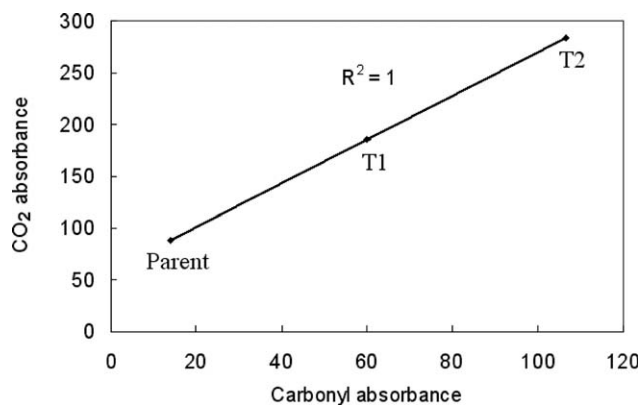


Figure 14 CO₂ absorbance after 3 h UV exposure versus carbonyl absorption after 465 h UVA340 exposure.

CONCLUSIONS

LDPE films formulated with nano-particulate TiO₂ were found to absorb UV wavelengths up to ~ 350 nm but retained good transmission in the visible range and had good optical clarity. When exposed in QUV equipment, the life of the TiO₂-containing films was still ~ 400 h, even though the presence of the TiO₂ reduced the time for which the film resisted cracking by about 50%.

The shortening of film life correlated with the rate of development of carbonyl absorption. In turn, this correlated well with the much more rapid measurement of CO₂ that was emitted as a degradation product. These measurements were not unduly perturbed by the presence of the additives used to disperse the TiO₂. Consequently, both the development of carbonyl absorption and the photogeneration of carbon dioxide may be used to assess the relative photostability of the different films. However, the speed of the FTIR CO₂ measurements has particular advantages as a screening method. This is of particular benefit for formulations in which interactions between inorganic particulate and stabilizers, such as antioxidants, are of potential concern.

References

1. Ray, S. S.; Okamoto, M. *Prog Polym Sci* 2003, 28, 1539.
2. Ellis, T. S.; D'Angelo, J. S. *J Appl Polym Sci* 2003, 90, 1639.
3. Ray, S. S.; Maiti, P.; Okamoto, M.; Yamada, K.; Ueda, K. *Macromolecules* 2002, 35, 3104.
4. Li, Y.; Yu, J.; Guo, Z. X. *Eng Plast Appl* 2002, 30, 7.
5. Mishra, S.; Sonawane, S. H.; Singh, R. P. *J Polym Sci Part B: Polym Phys* 2005, 43, 107.
6. Lloyd, S. M.; Lave, L. B. *Environ Sci Technol* 2003, 37, 3458.
7. Salahuddin, N.; Moet, A.; Hiltner, A.; Baer, E. *Eur Polym J* 2002, 38, 1477.
8. Morawiec, J.; Pawlak, A.; Slouf, M.; Galeski, A.; Piorkowska, E.; Krasnikowa, N. *Eur Polym J* 2005, 41, 1115.
9. Lai, S. M.; Li, H. C.; Liao, Y. C. *Eur Polym J* 2007, 43, 1660.
10. Cho, S. M.; Choi, W. Y. *J Photochem Photobiol A* 2001, 143, 221.
11. Hidaka, H.; Suzuki, Y.; Nohara, K.; Horikoshi, S.; Hisamatsu, Y.; Pelizzetti, E.; Serpone, N. *J Polym Sci Part A: Polym Chem* 1996, 34, 1311.
12. Horikoshi, S.; Serpone, N.; Hisamatsu, Y.; Hidaka, H. *Environ Sci Technol* 1998, 32, 4010.
13. Jin, C.; Christensen, P. A.; Egerton, T. A.; Lawson, E. J.; White, J. R. *Polym Degrad Stab* 2006, 91, 1086.
14. Allen, N. S.; Khatami, H.; Thompson, F. *Eur Polym J* 1992, 28, 817.
15. Allen, N. S.; Katami, H. *Polym Degrad Stab* 1996, 52, 311.
16. Allen, N. S.; Edge, M.; Sandoval, G.; Ortega, A.; Liauw, C. M.; Stratton, J.; McIntyre, R. B. *Polym Degrad Stab* 2002, 76, 305.
17. Allen, N. S.; Edge, M.; Ortega, A.; Sandoval, G.; Liauw, C. M.; Verran, J.; Stratton, J.; McIntyre, R. B. *Polym Degrad Stab* 2004, 85, 927.
18. Zeynalov, E. B.; Allen, N. S. *Polym Degrad Stab* 2006, 91, 931.
19. Zeynalov, E. B.; Allen, N. S. *Polym Degrad Stab* 2004, 86, 115.
20. Rabek, J. F. *Photostabilization of Polymers*; Elsevier Applied Science: London, 1990.
21. Jin, C.; Christensen, P. A.; Egerton, T. A.; White, J. R. *Mater Sci Technol* 2006, 22, 908.
22. Fernando, S. S.; Christensen, P. A.; Egerton, T. A.; White, J. R. *Polym Degrad Stab* 2007, 92, 2163.
23. Fernando, S. S.; Christensen, P. A.; Egerton, T. A.; White, J. R. *Polym Degrad Stab* 2009, 94, 83.
24. Fechine, G. J. M.; Christensen, P. A.; Egerton, T. A.; White, J. R. *Polym Degrad Stab* 2009, 94, 234.
25. Jin, C.; Christensen, P. A.; Egerton, T. A.; White, J. R. *Polymer* 2003, 44, 5969.
26. Egerton, T. A.; Everall, N. J.; Tooley, I. R. *Langmuir* 2005, 21, 3172.
27. Commereuc, S.; Vaillant, D.; Philippart, J. L.; Lacoste, J.; Lemaire, J.; Carlsson, D. J. *Polym Degrad Stab* 1997, 57, 175.
28. Gijsman, P.; Meijers, G.; Vitarelli, G. *Polym Degrad Stab* 1999, 65, 433.
29. Allen, N. S.; Edge, M.; Corrales, T.; Catalina, F. *Polym Degrad Stab* 1998, 61, 139.
30. Strandberg, C.; Albertsson, A. C. *J Appl Polym Sci* 2005, 98, 2427.
31. Delprat, P.; Duteurtre, X.; Gardette, J. L. *Polym Degrad Stab* 1995, 50, 1.